



This open access document is published as a preprint in the Beilstein Archives with doi: 10.3762/bxiv.2019.23.v1 and is considered to be an early communication for feedback before peer review. Before citing this document, please check if a final, peer-reviewed version has been published in the Beilstein Journal of Organic Chemistry.

This document is not formatted, has not undergone copyediting or typesetting, and may contain errors, unsubstantiated scientific claims or preliminary data.

Preprint Title Tautomerism as primary signalling mechanism in metal sensing: the case of amide group

Authors Vera V. Deneva, Georgi Dobrikov, Aurelien Crochet, Daniela Nedeltcheva, Katharina M. Fromm and Liudmil Antonov

Article Type Full Research Paper

Supporting Information File 1 BJOC_SI.docx; 60.5 KB

ORCID® IDs Vera V. Deneva - <https://orcid.org/0000-0002-1285-9037>; Georgi Dobrikov - <https://orcid.org/0000-0003-0437-2162>; Aurelien Crochet - <https://orcid.org/0000-0002-4763-2764>; Katharina M. Fromm - <https://orcid.org/0000-0002-1168-0123>; Liudmil Antonov - <https://orcid.org/0000-0003-0520-1517>

Tautomerism as primary signalling mechanism in metal sensing: the case of amide group

Vera Deneva*¹, Georgi Dobrikov¹, Aurelien Crochet², Daniela Nedeltcheva¹, Katharina M. Fromm² and Liudmil Antonov*¹

¹Institute of Organic Chemistry with Centre of Phytochemistry, Bulgarian Academy of Sciences, Sofia 1113, Bulgaria and ²University of Fribourg, Department of Chemistry, Chemin du Musée 9, CH-1700 Fribourg, Switzerland

* Corresponding authors e-mails: Liudmil Antonov – lantonov@orgchm.bas.bg; Vera Deneva - vdeneva@orgchm.bas.bg

Abstract

The concept for sensing systems using the tautomerism as elementary signaling process has been further developed by synthesizing a ligand containing 4-(phenyldiazenyl)naphthalene-1-ol as a tautomeric block and an amide group as metal capturing antenna. Although it has been expected, that the intramolecular hydrogen bonding (between the tautomeric hydroxyl group and the nitrogen atom from the amide group), could stabilize the pure enol form in some solvents, the keto tautomer is also observed. This is a result from formation of intramolecular associates in some solvents. Strong bathochromic and hyperchromic effects on the visible spectra accompany the complex 1:1 formation with some alkaline earth metal ions.

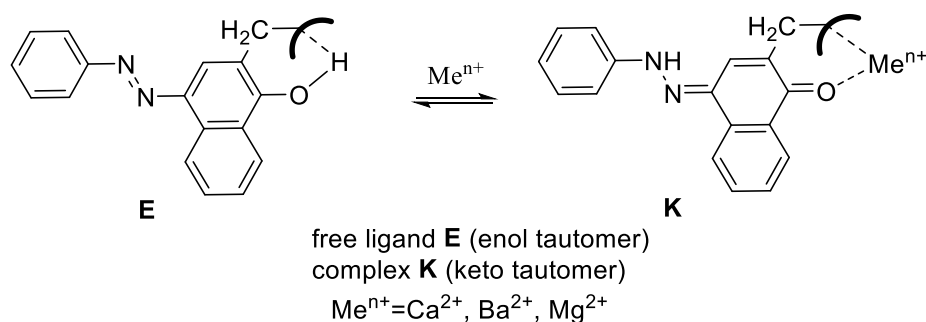
Keywords

tautomerism; molecular sensor; azo dye; amide group; sidearm

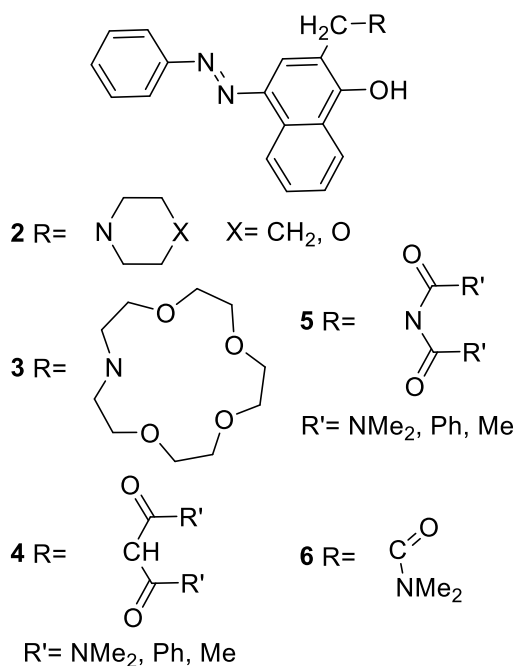
Introduction

The design of new organic sensing systems is undividable part of the development of coordination chemistry¹. Particular chromophore ligands as a complex have been successfully utilized for colorimetric detection of the majority of the metal ions². Some of them are used as standard tools in the chelatometric titrations³. The design of specific ligands for alkali metal determination is still a challenge. In the case of alkaline earth metal ions, the reagents with reasonable selectivity are still not commonly accepted, since they compete with the transitional metal ions⁴. The discovery of crown ethers⁵ and 3D based ligands⁶, unquestionably helped the development of natural ligand-supported metal investigation.

The ion recognitions based on existence of two molecular states (ligand and complex) with different optical properties and structure that allows fast transfer from the ligand to the complex upon addition of the desired metal ion⁷. The tautomeric proton exchange has the same properties when the equilibrium is switched from one to the other tautomer. The tautomerism can be controlled by metal ion addition, when a ionophore unit is implemented in the tautomeric backbone. The conceptual idea ^{7,8} is shown in Scheme 1, where the pure enol-like tautomeric form is achieved in the free ligand through an intramolecular hydrogen bonding, while the interaction with the metal ion ejects the tautomeric proton and stabilizes the corresponding tautomeric counter-form.



Scheme 1: Conceptual idea for tautomeric metal sensing.



Scheme 2: Tautomeric structures.

Several successful tautomeric ligands, based on 4-(phenyldiazenyl)naphthalen-1-ol (**1**)⁸ (**2** and **3**, Scheme 2) as a tautomeric unit have been developed by us. It has been found out that structures **2** and **3** exist in the neutral state solely as enol tautomers due to intramolecular hydrogen bonding involving the tautomeric hydroxyl group and the complexation shifts the equilibrium to the **K**-form. Although such systems exhibit 3D structure and as a result, show high stability constants upon complexation their selectivity is rather low, which can be attributed to their complexation features. Developing the systems further, leads to modification of the ionophore part by replacing the crown ether with other ionophores, such as done in **4**

and **5**. The quantum-chemical calculations for **4** and **5**, have demonstrated that the stable enol tautomers exist as intramolecular C=O . . . HO bonded system, while in the **K** forms the ionophore part action does not participate in hydrogen bonding and can be considered as a basic 2-alkyl substitution⁹. Consequently, the stabilization between the **E** and **K** form is a result of the competition between the strength of the hydrogen bonding in the enol tautomer and the effect of simple alkyl substitution in the keto form skeleton. The calculations also suggest that the efficient switching towards the enol form can be achieved only when R' = NMe₂ (Scheme 2).

Theoretical modelling of structures **4** and **5**, have also shown that only one of the carbonyl groups from the ionophore unit really participates in the capturing of the metal ion upon complexation¹⁰. Therefore, the aim of the current communication is to estimate theoretically and experimentally, the tautomeric state and complexation abilities of compound **6**, where only one carbonyl group in the ionophore part is present (Scheme 2). It is expected that the enol tautomer would be stabilized in the neutral state, due to the formation of strong intramolecular hydrogen bonding between the tautomeric OH group and the carbonyl group in the ionophore part. Upon complexation, depending on the size and charge of the metal ion, a complex formation should shift the tautomeric equilibrium towards the keto tautomer and should provide large stabilization of the complex. According to our best knowledge, such system has not been designed up to now.

Results and Discussion

Compound **1** is a well studied tautomeric structure featuring moderate energy gap between the enol **E** and the keto **K** tautomeric forms¹¹. For this reason, the tautomeric equilibrium can be easily affected by changing the solvent. As shown on Scheme 1a, the tautomeric equilibrium has not been switched fully to either of the

tautomers. For instance, the experimentally determined ΔG values at room temperature range from 1.42 kcal/mol, which corresponds to around 8% (in cyclohexane) or 10% (in methylcyclohexane/toluene) of the **K** tautomer^{12,13}, to -0.71 kcal/mol in chloroform, where this tautomer dominates. The ΔG value of 0.33 kcal/mol in acetonitrile, determined experimentally⁸, have been used to validate the level of theory used in the current study. As seen from Table S1 the best result has been achieved by using M06-2X/6-31++G**, which predicts relative energy of the tautomers (ΔE value, defined as $E_K - E_E$) of 0.33 kcal/mol, perfectly matching the experiment.

In the case of **6** the calculations yield a ΔE value of 3.14 kcal/mol in acetonitrile, which leads to expectation that the tautomeric equilibrium is fully shifted to **6E**. The corresponding most stable structure of the enol form is shown in Figure 1, where hydrogen bonding between the tautomeric OH group and the sidearm carbonyl group is seen.

The tautomeric equilibrium in **1** is strongly solvent-dependent as mentioned above and seen from Figure 2a. For instance, chloroform through intermolecular hydrogen bonding with the carbonyl oxygen atom from the tautomeric backbone, stabilizes the keto tautomer, absorbing at ~ 480 nm, while in acetonitrile the enol form is also presented with a maximum at ~ 410 nm.

A comparison between the absorption spectra of **1** and **6** shows that the tautomeric equilibrium in **6** is also surprisingly solvent dependent. As shown on Figure 2b, the tautomeric equilibrium in **6** is shifted towards the **K** form in acetonitrile, ethanol and chloroform and towards the **E** form in dichloromethane and toluene.

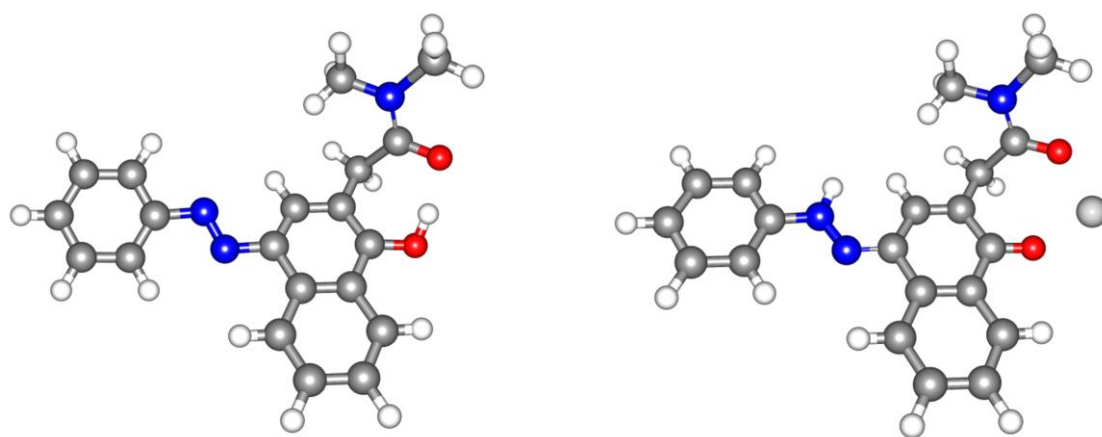


Figure 1: The most stable tautomeric form of **6** in neutral state (left) and upon complexation with Mg(ClO₄)₂ (right).

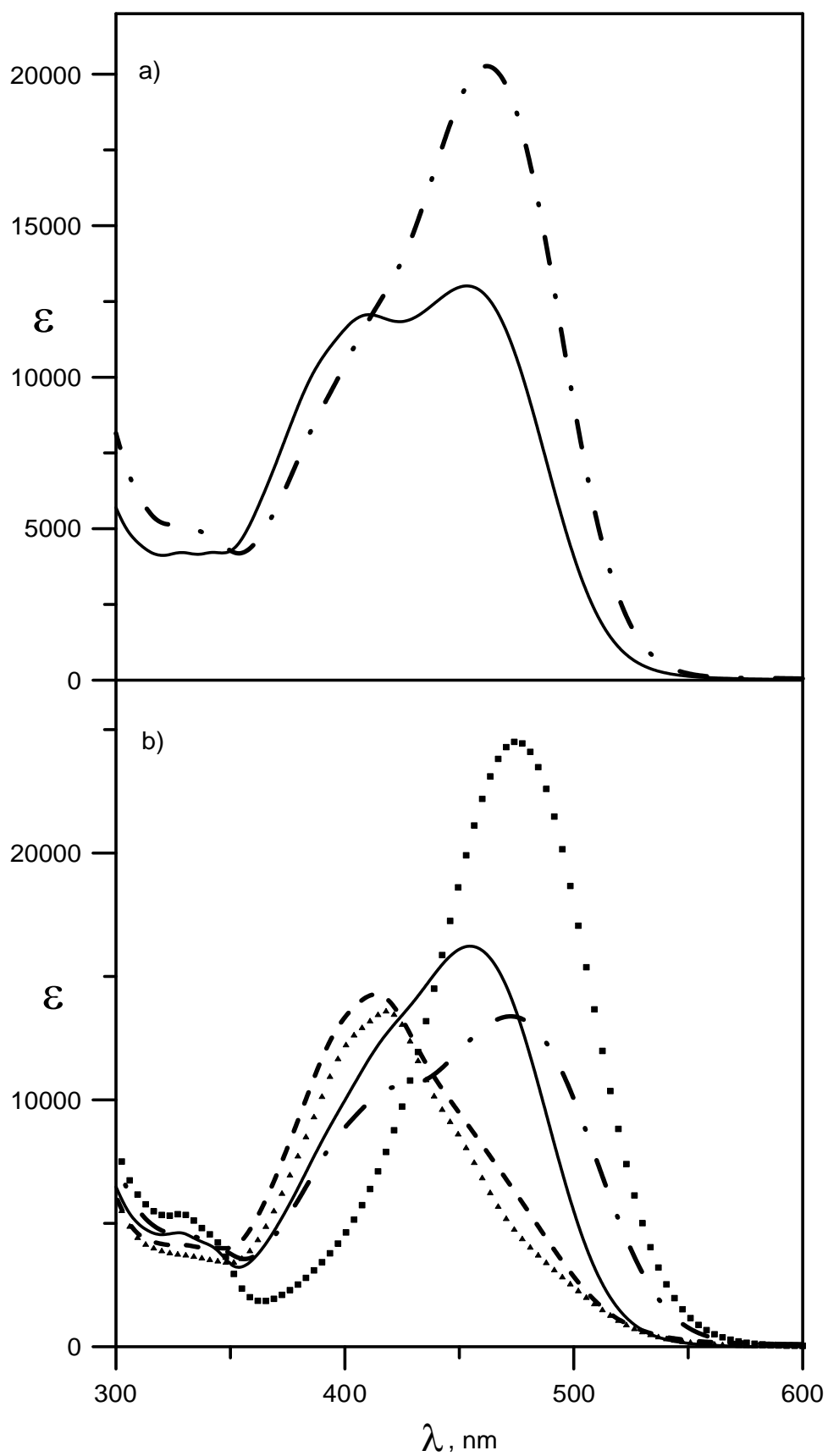


Figure 2: Absorption spectra of compounds **1** (a) and **6** (b) in acetonitrile (—), chloroform (— · —), dichloromethane (---), ethanol (■ ■ ■) and toluene (▲ ▲ ▲).

Having in mind the theoretical predictions discussed above, the existence of the keto tautomer in solution is surprising. This behavior might mean that either the enol stabilizing intramolecular H-bonding is not strong enough and can be broken by the solvent or there are intermolecular interactions not taken into account by the calculations. The explanation for the sudden stabilization of **6K** comes from the X-ray measurements of its crystal, obtained in acetonitrile. The crystal structure of **6**, shown in Figure 3, clearly indicates, that the **K** form is stabilized through formation of linear intermolecular associates. It is seen that the hydrogen bond is formed between the nitrogen proton of one keto tautomer and the carbonyl group of another neighboring molecule. Probably, the process of associate formation is facilitated by the position of the chromophore part in the isolated **K** form (Figure 3, left). Obviously, the formation of the seven-member hydrogen-bonding ring in **6E** cannot compete with the flexibility of the system in the case of the intermolecular association. Comparing to another tautomeric C=O containing ionophore, recently developed¹⁴, it seems that the existence of a carbonyl group leads in some cases to stabilization of the keto tautomer through formation of associates.

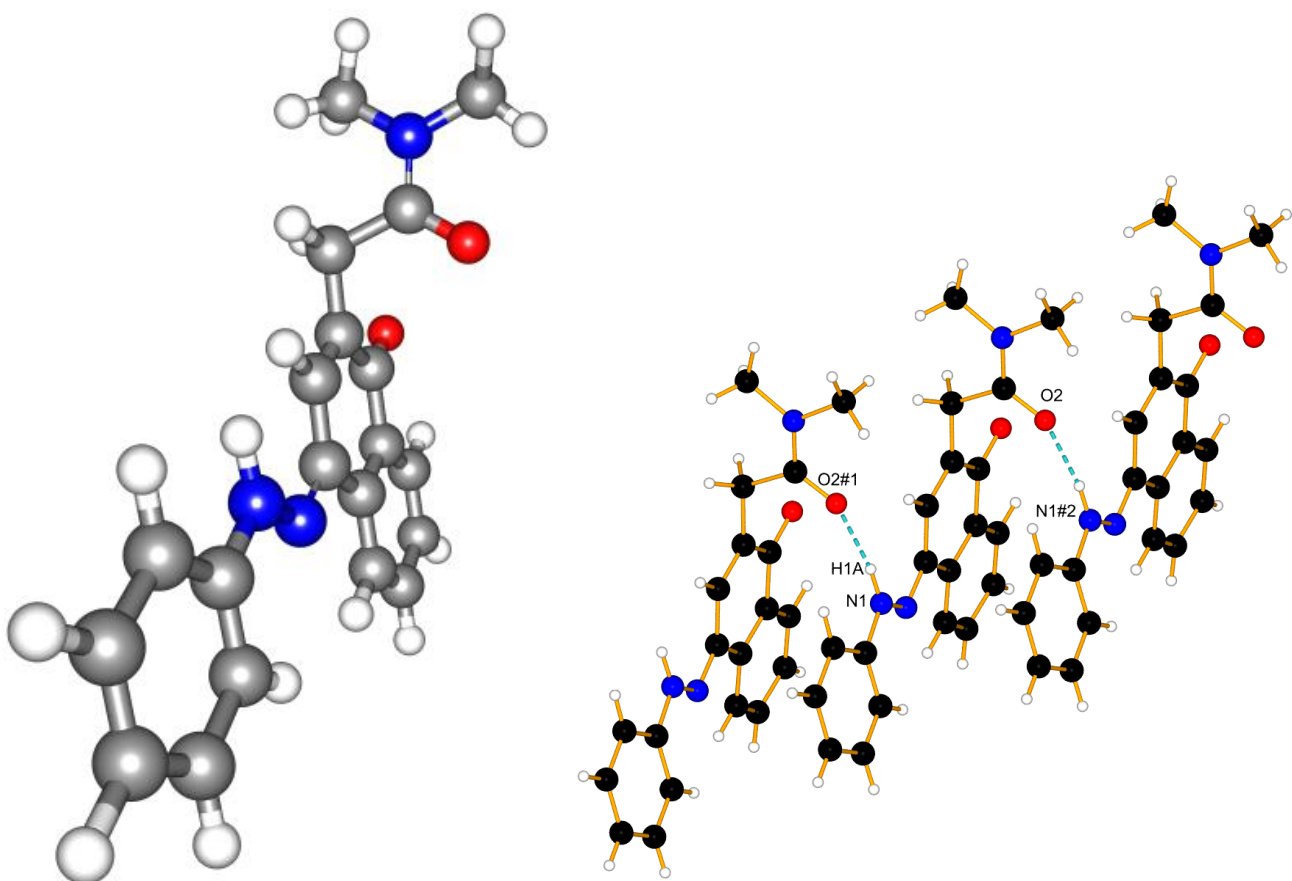


Figure 3. Theoretically predicted structure of **6K** (left). X-ray structure of **6** (right), #1: $x-1, y, z$; #2: $x+1, y, z$; H bonds are drawn as blue dash lines.

The absorption spectra of **6** in acetonitrile upon addition of $\text{Mg}(\text{ClO}_4)_2$ are shown on Figure 4. It is clear that the tautomeric equilibrium is shifted towards the keto tautomer as a result of the complexation, which provides substantial red shift (from 410 to 480 nm) comparing to the neutral ligand. At the same time increased intensity of the new maximum at 480 nm is observed. The comparison between the spectra of the complex and the deprotonated ligand, shown on Figure 4, indicates that the complex formation is not related to deprotonation and leads to shift in the tautomeric equilibrium. These results coincide with the results obtained for compound **3**¹⁵.

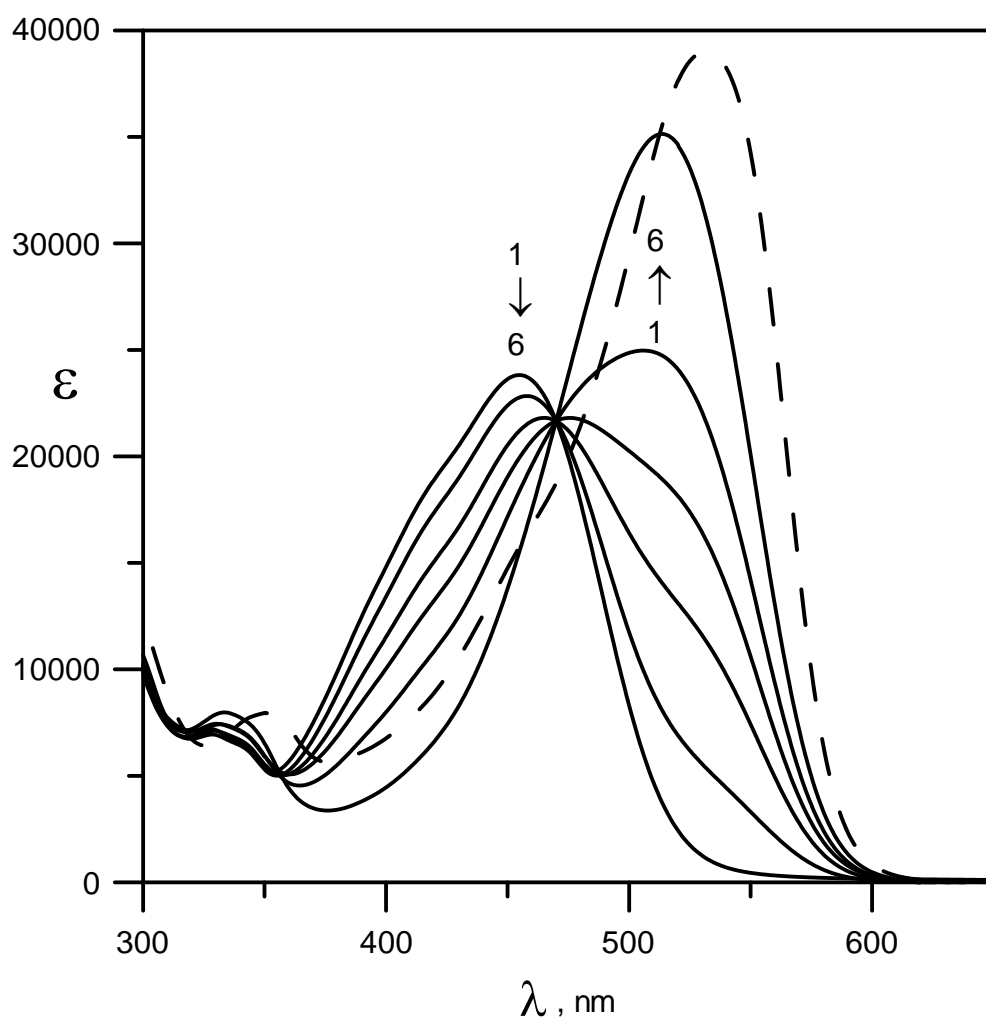


Figure 4. Absorption spectra of **6** with stepwise addition of $\text{Mg}(\text{ClO}_4)_2$ in acetonitrile (1-neutral ligand; 6-complex $C_{\text{Mg}(\text{ClO}_4)_2} = 1.23 \cdot 10^{-3}\text{M}$. The spectrum of the deprotonated form of **6** is given with dashes.

The complexation abilities of **6** towards some alkaline-earth metal ions were studied and the obtained spectra of the complexes are given in Figure 5, indicating the reached maximal concentrations of the corresponding salts (determined by their solubility in acetonitrile). It was observed that upon stepwise addition of the metal salts λ_{max} of the complex changes with the change of the metal ion type. We assume the formation of 1:1 complex (the Job's plots are shown on Figure S1), which leads to spectral shift of appr. 70 nm, which corresponds to the appearance of the keto

tautomer. This means that the metal ion interacts with the C=O group and stabilizes the **6K** form.

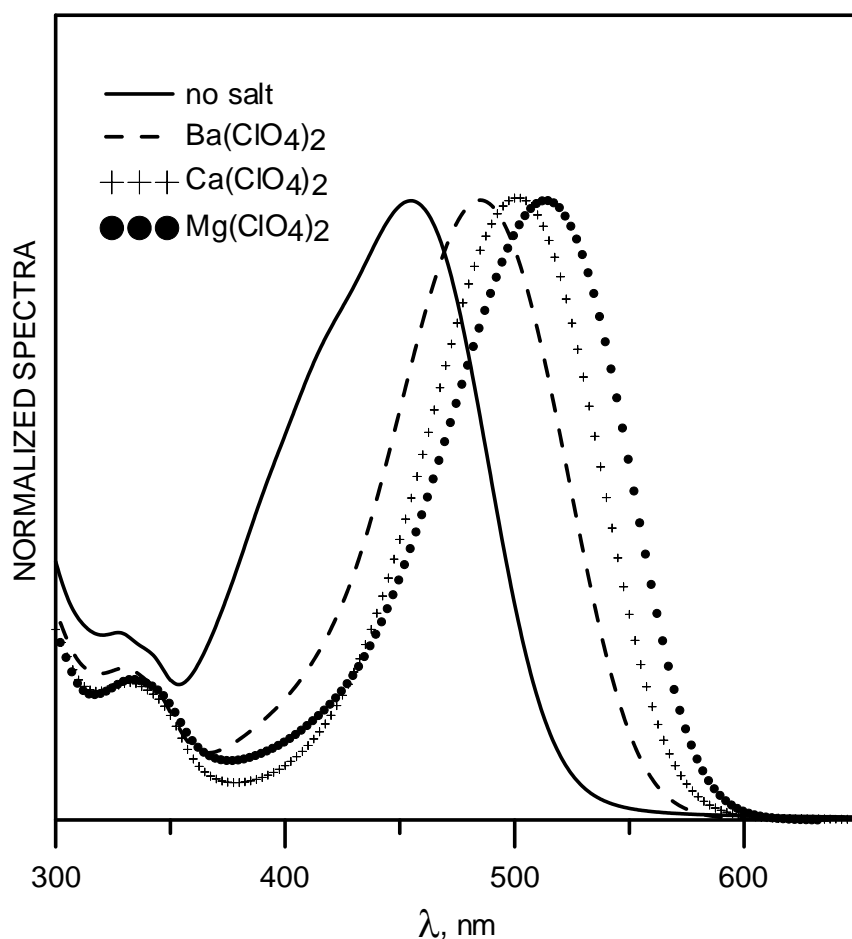


Figure 5. Normalized spectra of the free ligand **6** ($c= 5.10^{-5}M$) and its complexes obtained with Ba(ClO₄)₂, Ca(ClO₄)₂ and Mg(ClO₄)₂.

The estimated stability constants and the absorption spectra maxima of the complexes are summarized in Table 1. As seen, the complex formation causes substantial red shift, which varies with the metal ion. It is worth mentioning that complexation with any alkaline metals was not observed. As seen, **6** shows strong complexation with Ba²⁺, which fits well with the size of the cavity formed between the two carbonyl groups of the keto form of the ligand, while the corresponding stability constants with Ca²⁺ and Mg²⁺ are very similar. However, as seen from Figure 5 and

Table 1, the difference in the spectral maxima of the complexes allows detection of each of the studied cations.

Table 1: Absorption maxima of the complexes with different alkaline-earth metal ions and stability constants of the complexes of **6** in acetonitrile.

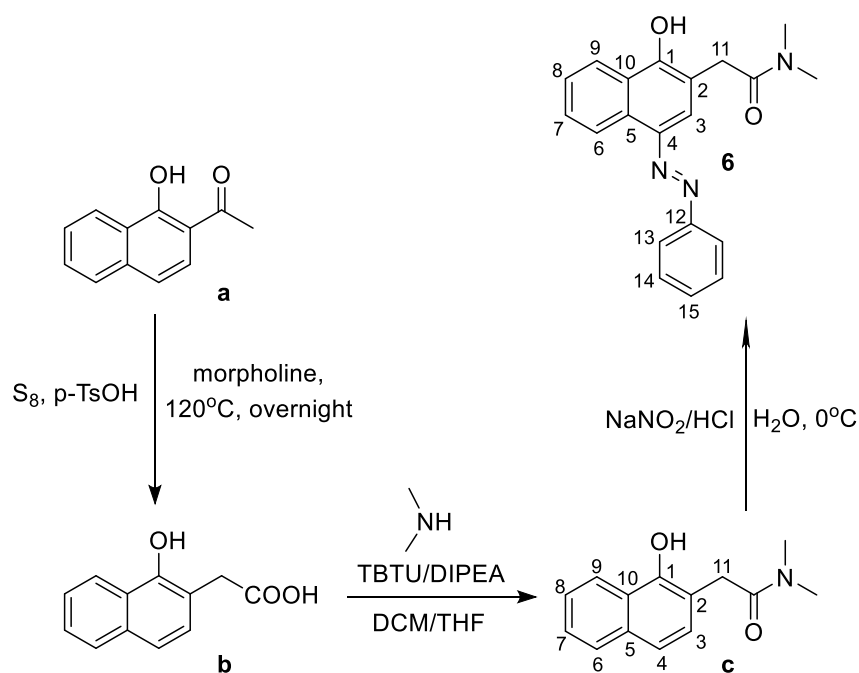
Metal ion	$\log \beta$	λ_{\max} complex, [nm]
Ba ²⁺	3.2±0.10	485
Ca ²⁺	2.8±0.04	500
Mg ²⁺	2.6±0.05	515

Conclusion

In the current study, we model theoretically and experimentally tautomerism and complexation abilities of a new tautomeric ligand, based on 4-(phenyldiazenyl)naphthalen-1-ol. The enol form stabilization could be achieved through strong intramolecular hydrogen bond formation between the tautomeric OH group and the carbonyl group from the tautomeric backbone, but also intermolecular association plays role in some solvents. The calculations predict that the complexation with alkali earth metal ions could lead to a full shift of the tautomeric equilibrium towards keto tautomer, which was observed in solution. The formed 1:1 complex shows large bathochromic shift.

Experimental

Organic synthesis



Preparation of compound **c**:

The starting intermediate **b** was prepared according described procedure¹⁶ from commercially available ketone **a**.

Compound **b** (1.22 g, 6.03 mmol) was suspended in 20 ml dry dichloromethane and this mixture was cooled to 0°C . Consequently, to this suspension were added dry diisopropylethylamine (6.3 ml, 36.20 mmol), TBTU (3.87 g, 12.07 mmol) and 2.0 M solution of dimethylamine in dry THF (6.0 ml, 12.07 mmol). The reaction mixture was stirred for 7 days at r.t. (reaction monitoring by TLC – dichloromethane:petroleum ether = 5:2). The reaction mixture was washed successively with aq. citric acid and water, dried over Na_2SO_4 , filtered and evaporated under vacuum. The crude product was purified by column chromatography - 75 g silica gel, phase dichloromethane:petroleum ether = 5:2, to give 0.59 g (43%) of pure **c** as beige crystals.

Data for compound **c**:

2-(1-hydroxynaphthalen-2-yl)- N,N -dimethylacetamide

m.p. 87-88°C. ^1H NMR (600.11 MHz, CDCl_3 , 293 K): δ = 8.36 (m, 1H, H-9), 7.74 (m, 1H, H-6), 7.45 (m, 2H, H-7, H-8), 7.33 (d, 1H, H-4, J = 8.3 Hz), 7.13 (d, 1H, H-3, J = 8.3 Hz), 3.87 (s, 2H, H-11), 3.23 (s, 3H, N- CH_3), 2.98 (s, 3H, N- CH_3). ^{13}C NMR (150.90 MHz, CDCl_3 , 293 K): δ = 173.44 (1C, $\text{C}=\text{O}$), 153.26 (1C, C-1), 134.02 (2C, C-5, C-10), 128.09 (1C, C-3), 127.05 (1C, C-6), 126.18 (1C, C-7), 125.13 (1C, C-8), 122.74 (1C, C-9), 119.30 (1C, C-4), 113.11 (1C, C-2), 38.48 (1C, N- CH_3), 36.89 (1C, C-11), 35.95 (1C, N- CH_3). Anal. calc. for $\text{C}_{14}\text{H}_{15}\text{NO}_2$ (229.11): C, 73.34; H, 6.59; N, 6.11. Found: C, 73.25; H, 6.68; N, 6.03 %.

Preparation of compound **6**:

Preparation of phenyldiazonium salt solution: Aniline (0.90 ml, 10.00 mmol) was dissolved in a mixture of concentrated hydrochloric acid (5 mL) and distilled water (20 mL). A solution of sodium nitrite (0.83 g, 12.00 mmol) in distilled water (5 mL) was prepared in a test tube. Sodium nitrite solution was added dropwise to the acidic solution of amine over 5 min at 0°C. The mixture was stirred at 0°C for 40 min. Compound **c** (0.59 g, 2.57 mmol) was dissolved in aqueous solution of NaOH (1.03 g, 25.73 mmol in 10 ml distilled water) and cooled to 0°C. The above prepared phenyldiazonium salt solution (6.43 ml, 2.57 mmol) was added dropwise to the solution of **c** at 0°C. The resultant deep red mixture was stirred for 1 h at 0°C. The crude product **6** was precipitated by addition of 20% hydrochloric acid, filtered and washed with distilled water. For further purification the crude product was dissolved in 5 ml dichloromethane and purified by column chromatography - 75 g silica gel, phase dichloromethane:methyl-tert-butyl ether = 10:1. After column, the product was additionally washed with petroleum ether and dried in vacuum to give 0.720 g (84%) of pure **6** as bright red crystals.

Data for compound **6**:

(E)-2-(1-hydroxy-4-(phenyldiazenyl)naphthalen-2-yl)-N,N-dimethylacetamide

m.p. 152-153°C. ¹H NMR* (600.11 MHz, DMSO-d⁶ with 1.5 eq. excess of NaOH, 293 K): δ = 11.51 (br s, 1H, OH), 8.50 (br d, 1H, H-9, J =), 8.10 (br s, 1H, H-3), 8.07 (br d, 1H, H-6, J =), 7.68 (m, 1H, H-8), 7.59 (m, 2H, H-13), 7.50 (m, 1H, H-7), 7.42 (m, 2H, H-14), 7.10 (m, 1H, H-15), 3.64 (s, 2H, H-11), 3.12 (s, 3H, N-CH₃), 2.85 (s, 3H, N-CH₃). ¹³C NMR* (150.90 MHz, DMSO-d⁶ with 1.5 eq. excess of NaOH, 293 K): δ = 169.84 (1C, C=O), 135.31 (2C, C-5, C-10), 130.94 (br s, 1C, C-8), 129.41 (2C, C-14), 128.63 (br s, 1C), 126.71 (br s, 1C, C-7), 125.06 (1C, C-6), 123.67 (br s, 1C, C-15), 122.46 (1C, C-9), 115.98 (br s, 2C, C-13), 112.36 (1C, C-2), 37.16 (1C, N-CH₃), 35.07 (1C, N-CH₃), 34.70 (1C, C-11). Anal. calc. for C₂₀H₁₉N₃O₂ (333.39): C, 72.05; H, 5.74; N, 12.60. Found: C, 72.12; H, 5.70; N, 12.67 %. MS (HR) m/z (rel. int.): 333.14649 (-2.05527 ppm).

* Due to tautomerism, the NMR spectra in most of the solvents (DMSO-d⁶, CDCl₃, acetone-d⁶, acetonitrile-d³ etc.) are not informative. In all cases a complicated mixture of tautomers and lack of signals was observed. Therefore, the NMR spectra were recorded in strong basic media, in order to obtain single tautomer.

Nevertheless, some signals in ¹³C NMR spectra do still not exist even after 1024 scans.

Theoretical calculations

Quantum-chemical calculations were performed using the Gaussian 09 D.01 program suite¹⁷. The M06-2X functional^{18,19} was used with the 6-31++G** basis set for the calculations. This fitted hybrid meta-GGA functional with 54% HF exchange was especially developed to describe main-group thermochemistry and non-covalent interactions. It shows very good results in predicting the position of tautomeric

equilibria for compounds with intramolecular hydrogen bonds as well as describing ground and excited state proton transfer mechanism^{20–25}.

The solvent effect of the solvents was described using the Polarizable Continuum Model (the integral equation formalism variant, IEFPCM, as implemented in Gaussian 09)²⁶. All ground state structures were optimized without restrictions, using tight optimization criteria and an ultrafine grid in the computation of two-electron integrals and their derivatives. The true minima were verified by performing frequency calculations in the corresponding environment. The TD-DFT method^{27–29}, carried out with the same functional and basis set, was used for predicting vertical transitions.

Spectral measurements

The NMR spectra were recorded on a Bruker Avance II+ 600 spectrometer. In case of CDCl₃ tetramethylsilane was used as internal standard. In case of DMSO-d⁶, the spectra were calibrated to the residual solvent peaks (for DMSO-d⁶: δ =2.50 for 1H). ¹³C spectra were calibrated in all cases to the residual solvent peaks (for CDCl₃ δ =77.00, for DMSO-d⁶ δ =39.52). The following additional NMR techniques were used for all compounds: DEPT 135, COSY, HSQC and HMBC. Mass spectra (MS) were recorded on a Thermo Scientific High Resolution Magnetic Sector MS DFS. UV–Vis spectral measurements were performed on a Jasco V-570 UV–Vis–NIR spectrophotometer, equipped with a thermostatic cell holder (using Huber MPC-K6 thermostat with 1°C precision) in spectral grade solvents at 20°C. The complexation was studied in acetonitrile. AR grade Mg(ClO₄)₂ (Fluka), Ca(ClO₄)₂·4H₂O (Aldrich) and Ba(ClO₄)₂·aq (Fluka) were vacuum dried at 90°C for 3 days. Due to the red shift upon complexation, the estimation of the stability constants was performed at the maximum of the complex using the final complex spectrum (Figure 5). Deprotonation was made with trimethylamine (Aldrich).

X-ray crystallographic measurements

Experimental

Single crystals of **6** were crystallized from acetonitrile by slow evaporation. A suitable crystal was selected and was mounted on a loop in oil on a Stoe IPDS2T diffractometer. The crystallographic data of single crystal were collected with Cu K α ₁ radiation ($\lambda = 1.54186 \text{ \AA}$). The crystal was kept at 250(2) K during data collection by an Oxford Cryosystem open-flow cryostats. Using Olex2³⁰, the structure was solved with the ShelXT³¹ structure solution program using Intrinsic Phasing and refined with the ShelXL³¹ refinement package using Least Squares minimization.

Crystal structure determination of **6**

Crystal Data for C₂₀H₁₉N₃O₂ ($M = 333.38 \text{ g/mol}$): monoclinic, space group $P2_1/c$ (no. 14), $a = 5.5438(8) \text{ \AA}$, $b = 17.850(2) \text{ \AA}$, $c = 17.184(3) \text{ \AA}$, $\beta = 91.719(12)^\circ$, $V = 1699.7(4) \text{ \AA}^3$, $Z = 4$, $T = 250(2) \text{ K}$, $\mu(\text{CuK}\alpha) = 0.691 \text{ mm}^{-1}$, $d_{\text{calc}} = 1.303 \text{ g/cm}^3$, 14285 reflections measured ($7.142^\circ \leq 2\theta \leq 135.89^\circ$), 2929 unique ($R_{\text{int}} = 0.0894$, $R_{\text{sigma}} = 0.0584$) which were used in all calculations. The final R_1 was 0.0627 ($I > 2\sigma(I)$) and wR_2 was 0.1642 (all data). CIF file can be obtained from the Cambridge Crystallographic Data Centre: CCDC-1914884 (**6**).

Supporting Information

Supporting information can be found in File SI.

Acknowledgements

This work was supported by Bulgarian National Science Fund [Grant Number DFNI DM09/6 and DCOST 01/05/2017].

References

- (1) Lawrance, G. A. *Introduction to Coordination Chemistry*; John Wiley & Sons, Ltd: Chichester, UK, 2010. <https://doi.org/10.1002/9780470687123>.

- (2) Lee, B. Review of the Present Status of Optical Fiber Sensors. *Optical Fiber Technology* **2003**, 9 (2), 57–79. [https://doi.org/10.1016/S1068-5200\(02\)00527-8](https://doi.org/10.1016/S1068-5200(02)00527-8).
- (3) Hildebrand, G. P.; Reilley, C. N. New Indicator for Complexometric Titration of Calcium in Presence of Magnesium. *Analytical Chemistry* **1957**, 29 (2), 258–264. <https://doi.org/10.1021/ac60122a025>.
- (4) *Host Guest Complex Chemistry / Macrocycles*; Vögtle, F., Weber, E., Eds.; Springer Berlin Heidelberg: Berlin, Heidelberg, 1985. <https://doi.org/10.1007/978-3-642-70108-5>.
- (5) Pedersen, C. J. The Discovery of Crown Ethers. *Science* **1988**, 241 (4865), 536–540. <https://doi.org/10.1126/science.241.4865.536>.
- (6) Gokel, G. W.; Dishong, D. M.; Diamond, C. J. Lariat Ethers. Synthesis and Cation Binding of Macrocyclic Polyethers Possessing Axially Disposed Secondary Donor Groups. *Journal of the Chemical Society, Chemical Communications* **1980**, No. 22, 1053. <https://doi.org/10.1039/c39800001053>.
- (7) *Tautomerism: Methods and Theories*; Antonov, L., Ed.; Wiley-VCH: Weinheim, 2014.
- (8) Antonov, L.; Deneva, V.; Simeonov, S.; Kurteva, V.; Nedeltcheva, D.; Wirz, J. Exploiting Tautomerism for Switching and Signaling. *Angewandte Chemie International Edition* **2009**, 48 (42), 7875–7878. <https://doi.org/10.1002/anie.200903301>.
- (9) Deneva, V.; Antonov, L. Attaching Tweezers like Ionophore to a Proton Crane: Theoretical Design of New Tautomeric Sensors. *Molecular Physics* **2019**, 1–8. <https://doi.org/10.1080/00268976.2018.1562127>.
- (10) *Tautomerism: Methods and Theories*; Antonov, L., Ed.; Wiley-VCH: Weinheim, 2014.
- (11) Antonov, L.; Kurteva, V.; Crochet, A.; Mirolo, L.; Fromm, K. M.; Angelova, S. Tautomerism in 1-Phenylazo-4-Naphthols: Experimental Results vs Quantum-Chemical Predictions. *Dyes and Pigments* **2012**, 92 (1), 714–723. <https://doi.org/10.1016/j.dyepig.2011.06.026>.
- (12) Dubonosov, A. D.; Minkin, V. I.; Bren, V. A.; Shepelenko, E. N.; Tsukanov, A. V.; Starikov, A. G.; Borodkin, G. S. Tautomeric Crown-Containing Chemosensors for Alkali-Earth Metal Cations. *Tetrahedron* **2008**, 64 (14), 3160–3167. <https://doi.org/10.1016/j.tet.2008.01.096>.
- (13) Joshi, H.; Kamounah, F. S.; van der Zwan, G.; Gooijer, C.; Antonov, L. Temperature Dependent Absorption Spectroscopy of Some Tautomeric Azo Dyes and Schiff Bases. *Journal of the Chemical Society, Perkin Transactions 2* **2001**, No. 12, 2303–2308. <https://doi.org/10.1039/b106241g>.
- (14) Kurteva, V. B.; Antonov, L. M.; Nedeltcheva, D. V.; Crochet, A.; Fromm, K. M.; Nikolova, R. P.; Shivachev, B. L.; Nikiforova, M. S. Switching Azonaphthols Containing a Side Chain with Limited Flexibility. Part 1. Synthesis and Tautomeric Properties. *Dyes and Pigments* **2012**, 92 (3), 1266–1277. <https://doi.org/10.1016/j.dyepig.2011.07.013>.
- (15) Antonov, L. M.; Kurteva, V. B.; Simeonov, S. P.; Deneva, V. V.; Crochet, A.; Fromm, K. M. Tautocrowns: A Concept for a Sensing Molecule with an Active Side-Arm. *Tetrahedron* **2010**, 66 (24), 4292–4297. <https://doi.org/10.1016/j.tet.2010.04.049>.
- (16) Neyyappadath, R. M.; Cordes, D. B.; Slawin, A. M. Z.; Smith, A. D. 6-Exo-Trig Michael Addition-Lactonizations for Catalytic Enantioselective Chromenone Synthesis. *Chemical Communications* **2017**, 53 (17), 2555–2558. <https://doi.org/10.1039/C6CC10178J>.

- (17) Frisch, M. J.; Trucks, G. W.; Schlegel, H. B.; Scuseria, G. E.; Robb, M. A.; Cheeseman, J. R.; Scalmani, G.; Barone, V.; Mennucci, B.; Petersson, G. A.; et al. *Gaussian 09 Revision D.01*; Gaussian, Inc.: Wallingford, CT, USA, 2013.
- (18) Zhao, Y.; Truhlar, D. G. Density Functionals with Broad Applicability in Chemistry. *Accounts of Chemical Research* **2008**, *41* (2), 157–167. <https://doi.org/10.1021/ar700111a>.
- (19) Zhao, Y.; Truhlar, D. G. The M06 Suite of Density Functionals for Main Group Thermochemistry, Thermochemical Kinetics, Noncovalent Interactions, Excited States, and Transition Elements: Two New Functionals and Systematic Testing of Four M06-Class Functionals and 12 Other Functionals. *Theoretical Chemistry Accounts* **2008**, *120* (1–3), 215–241. <https://doi.org/10.1007/s00214-007-0310-x>.
- (20) Kawauchi, S.; Antonov, L. Description of the Tautomerism in Some Azonaphthols. *Journal of Physical Organic Chemistry* **2013**, *26* (8), 643–652. <https://doi.org/10.1002/poc.3143>.
- (21) Manolova, Y.; Kurteva, V.; Antonov, L.; Marciniak, H.; Lochbrunner, S.; Crochet, A.; Fromm, K. M.; Kamounah, F. S.; Hansen, P. E. 4-Hydroxy-1-Naphthaldehydes: Proton Transfer or Deprotonation. *Physical Chemistry Chemical Physics* **2015**, *17* (15), 10238–10249. <https://doi.org/10.1039/C5CP00870K>.
- (22) Manolova, Y.; Marciniak, H.; Tschierlei, S.; Fennel, F.; Kamounah, F. S.; Lochbrunner, S.; Antonov, L. Solvent Control of Intramolecular Proton Transfer: Is 4-Hydroxy-3-(Piperidin-1-Ylmethyl)-1-Naphthaldehyde a Proton Crane? *Physical Chemistry Chemical Physics* **2017**, *19* (10), 7316–7325. <https://doi.org/10.1039/C7CP00220C>.
- (23) Hristova, S.; Dobrikov, G.; Kamounah, F. S.; Kawauchi, S.; Hansen, P. E.; Deneva, V.; Nedeltcheva, D.; Antonov, L. 10-Hydroxybenzo[h]Quinoline: Switching between Single- and Double-Well Proton Transfer through Structural Modifications. *RSC Advances* **2015**, *5* (124), 102495–102507. <https://doi.org/10.1039/C5RA20057A>.
- (24) Marciniak, H.; Hristova, S.; Deneva, V.; Kamounah, F. S.; Hansen, P. E.; Lochbrunner, S.; Antonov, L. Dynamics of Excited State Proton Transfer in Nitro Substituted 10-Hydroxybenzo[h]Quinolines. *Physical Chemistry Chemical Physics* **2017**, *19* (39), 26621–26629. <https://doi.org/10.1039/C7CP04476C>.
- (25) Hristova, S.; Deneva, V.; Pittelkow, M.; Crochet, A.; Kamounah, F. S.; Fromm, K. M.; Hansen, P. E.; Antonov, L. A Concept for Stimulated Proton Transfer in 1-(Phenyldiazenyl)Naphthalen-2-Ols. *Dyes and Pigments* **2018**, *156*, 91–99. <https://doi.org/10.1016/j.dyepig.2018.03.070>.
- (26) Tomasi, J.; Mennucci, B.; Cammi, R. Quantum Mechanical Continuum Solvation Models. *Chemical Reviews* **2005**, *105* (8), 2999–3094. <https://doi.org/10.1021/cr9904009>.
- (27) Improta, R. UV-Visible Absorption and Emission Energies in Condensed Phase by PCM/TD-DFT Methods. In *Computational Strategies for Spectroscopy*; Barone, V., Ed.; John Wiley & Sons, Inc.: Hoboken, NJ, USA, 2011; pp 37–75. <https://doi.org/10.1002/9781118008720.ch1>.
- (28) Adamo, C.; Jacquemin, D. The Calculations of Excited-State Properties with Time-Dependent Density Functional Theory. *Chemical Society Reviews* **2013**, *42* (3), 845–856. <https://doi.org/10.1039/c2cs35394f>.
- (29) Antonov, L.; Kawauchi, S.; Okuno, Y. Prediction of the Color of Dyes by Using Time-Dependent Density Functional Theory. *Bulgarian Chemical Communications* **2014**, *46* (A), 228–237.

- (30) Dolomanov, O. V.; Bourhis, L. J.; Gildea, R. J.; Howard, J. A. K.; Puschmann, H. *OLEX2*: A Complete Structure Solution, Refinement and Analysis Program. *Journal of Applied Crystallography* **2009**, *42* (2), 339–341. <https://doi.org/10.1107/S0021889808042726>.
- (31) Sheldrick, G. M. *SHELXT* – Integrated Space-Group and Crystal-Structure Determination. *Acta Crystallographica Section A Foundations and Advances* **2015**, *71* (1), 3–8. <https://doi.org/10.1107/S2053273314026370>.